Defensive Architecture of the Mediterranean. XV to XVIII centuries / Vol V/ González Avilés (Ed.)

Petrographic, geochemical and physical characterization of volcanic rocks from the fortification of Bosa Castle (western Sardinia, Italy)

***Stefano Columbu[a], Fabio Sitzia[a]**

[a]Dept. of Chemical and Geological Sciences, University of Cagliari, Italy, columbus@unica.it (*corresponding author)

Abstract

The fortification of Bosa Castle overlooking the valley of the river Temo and the medieval old town of Bosa (XII-XIV centuries). His tactical position militarily, which allowed control of the land from the sea to the river, setting up urban in the valley (*Bosa Vetus*), allowed the exploitation for centuries, even as a place of sighting to face sudden attacks of brigands or Saracen enemies. The site initially belonged to the *Giudicato di Torres* (around the X cent.), And finally twelve hundred to Malaspina (from Lunigiana). Later the castle suffered many renovations of Turrritani, Malaspina, Arborea, the Aragonese, although overall preserves the defensive structure built by the Marquis of Tuscany and Liguria. Its decline began in the second half of the sixteenth century in favor of nearby Alghero populated by Catalans.

This research proposal intends to define the petrographical and physical features and the weathering alteration of geomaterial used for the castle. The study of petro-volcanological features (*i.e*. structure, sialic and mafic minerals, welding degree) by macroscopic observations is the starting point for preliminary recognition of the different stones. Then, the analysis of texture and paragenesis on thin section by optical observations are made. Laboratory tests have been conducted to evaluate the physical-mechanical properties (density, water-absorption, porosity, PLT punching index, compressive and traction strength). The mapping of alteration forms and the causes of decay, in relation to varying volcanites and microclimatic-environmental conditions, have been studied.

Keywords: Medieval fortifications, Castle of Bosa, Physical features, Petrographic features.

1. Introduction

Serravalle Castle (Bosa, Italy), located on the top of the homonymous hill, is one of the most famous medieval fortifications of Sardinia (Fig. 1). The construction of the oldest nucleus, in the opinion of the historian Fara, is attributable to the Marquis Malaspina and to their arrival in Sardinia in 1112 AD (Fara 1543; Fiori 1995). In 1831 Vittorio Angius observed that the original fortification was much smaller than the present one but was later expanded in Aragonese period (Angius 1831; Soddu 2005; Spanu 1981).

In 1892 Fara supports the argument that Malaspina had founded a new settlement center on the slopes of Serravalle hill on which they built a fortress (Scano 1936). From the Aragonese period, the castle was expanded, strengthened and further protected to emphasize the defensive role played by the structure in the following centuries (Guagnini 1973). From an architectural point of view, the complex was built in 3 phases starting in 12th century. The first phase happened with the realization of 4 cantonial towers (with height of about 10 meters) with inner interposed wall (Fig. 2). The second phase concerns the construction of the main tower of the perimeter, the overhanging of

the walls and the creation of a second wall structure forming a trapezium. Other important additions to the later phase are identified in the construction of embankments and the St. Giovanni church. The decadence of the castle is already documented in 1571.

Fig. 1- The castle of Malaspina with pentagonal tower on the right (Bosa, Italy)

Fig. 2- Inner interposed walls with pentagonal tower on the left

Only in 1575 the problem was discussed in Spanish parliament where citizens urged urgent interventions to restore the castle's masonry. In the last century, the city walls were demolished and began, according to the indications of the current urban planning tools, the development towards the sea. At that time, the castle affected by two restoration works by Filippo Vivanet and Dionigi Scano in 1893, which predominantly interested the main tower.
In the present century, the castle was subjected to numerous restoration works carried out by the Sassari Superintendence with the aim of replacing some ashlars of the pentagonal tower irremediably altered (Columbu & Meloni 2015).

The last restoration projects started in 1999 and continued until 2005 and were joined by archaeological excavations inside the walls that allowed new discoveries that seem to change the history of the castle, today still very uncertain.

2. Geographical and geological background

The area of the castle site is mapped in 497 sheet (sections 1, 2, 3, 4) of Italian Map in 1:25.000 scale, and in 497050, 497060, 497070, 497100 and 497110 sheets of *Carta Tecnica Regionale* (CTR) in 1:10.000 scale. The sector consists of geological formations of tertiary/quaternary age, resting on the substrate represented by the Sardinian-Corsican crystalline basement.
The oldest formations are related to the late Oligocene represented by base volcanic rocks, attributable to intense Cainozoic volcanic activity, on which marine lacustrine tuffs stand on. Follow marine sediments related to Miocene transgression that affected the whole central-western part of the island. Pliocene and Quaternary are represented respectively by basaltic plateaux, derelict sediments of Tyrrhenian transgression along the coast, recent sands and valley-floods related to Temo and Turas rivers.

3. Sampling and analytical methods

Sampling was carried out according to the NORMAL Recommendations (Doc. N^{o} 3/80). Sampling points have been chosen taking into account the need to not disfigure the monument in any way. In addition, sampling was performed taking into account the most representative and/or predominant lithotypes in the entire architectural structure.
For physical tests, cubic specimens (dimensions 1.5x1.5x1.5 mm) were dried at 105 ± 5°C and the dry solid mass (m_D) was determined. The solid phases volume (V_S) of powdered rock specimens (on 5-8 g and with particle size less than 0.063 mm) and the real volume (with $V_R = V_S + V_C$ where V_C is the volume of pores closed to helium) of the rock specimens were determined by helium Ultrapycnometer 1000

(Quantachrome Instruments). The wet solid mass (m_W) of the samples was determined after water absorption by immersion for ten days. Through a hydrostatic analytical balance, the bulk volume V_B (with $V_B = V_S + V_O + V_C$ where $V_O = (V_B-V_R)$ is the volume of open pores to helium) is calculated as: $V_B = [(m_W-m_{HY})/\rho_W T_X]100$, where m_{HY} is the hydrostatic mass of the wet specimen and $\rho_W T_X$ is the water density at a temperature T_X. Total porosity (P_T), open porosity to water and helium ($\Phi_O H_2O$; $\Phi_O He$, respectively), closed porosity to water and helium ($\Phi_C H_2O$; $\Phi_C He$), bulk (ρ_B), real (ρ_R) and solid (ρ_S) densities are computed as:

$\Phi_T=[(V_B-V_S)/V_B]100$

$\Phi_O H_2O = \{[(m_W-m_D)/ \rho_W T_X]/V_B\}100$

$\Phi_O He = [(V_B-V_R)/V_B]100$

$\Phi_C H_2O = \Phi_T - \Phi_O H_2O$

$\Phi_C He = \Phi_T - \Phi_O He;$

$\rho_S = m_D/V_S;\ \rho_R = m_D/V_R;\ \rho_B = m_D/V_B$

The weight imbibition coefficient (CI_W) and the saturation index (SI) were computed as:

$CI_W = [(m_W-m_D)/m_D]100$

$SI = (\Phi_O H_2O/\Phi_O He) = \{[(m_W-m_D)/ \delta_W T_X]/V_O\}100$

The punching strength index was determined with a Point Load Tester (mod. D550 Controls Instrument) according to the International Society for Rock Mechanics (1972; 1985) on the same cubic rock specimens used for other physical properties. The resistance to puncturing (I_S) was calculated as $2\,P/D_e$, where P is the breaking load and D_e is the "equivalent diameter of the carrot", with $D_e = 4A/\pi$ and $A = WD$, where W and 2L are the width perpendicular to the direction of the load and the length of the specimen, respectively. The index value is referred to a standard cylindrical specimen with diameter D = 50 mm for which I_S has been corrected with a shape coefficient (F) and calculated as: $I_{S(50)} = I_S F = I_S(D_e/50)^{0.45}$.

The mineralogical and petrographic analysis of volcanic rocks were performed on thin sections under the polarizing microscope (Zeiss photomicroscope Pol II). The chemical composition of volcanic rock samples from field outcrops and the site were determined with a X-ray fluorescence spectrometer (XRF) Philips PW1400 with a Rh tube to analyse the major elements and some trace elements (Rb, Sr, Pb, Zn, Y, Nb, Zr), and with a W tube to analyse of Ni, Cr, Ba, V, La, Ce. Data reduction of major elements was performed by the method of Franzini et alii (1975, 1972). Data reduction of trace elements was performed by the method of Criss. The measurement accuracy is ± 1% for SiO_2, TiO_2, Al_2O_3, Fe_2O_3, CaO, K_2O and MnO and ± 4% for MgO, Na_2O and P_2O_5. Detection limits are about 3 ppm to 3σ for most of the elements; the accuracy of trace elements is ± 2 ÷ 3% to 1000 ppm; ± 5 ÷ 10% at 100 ppm and ± 10 ÷ 20% to 10 ppm. The weight loss for calcination (L.o.I., Lost on Ignition) was determined by calculating the loss in wt% at 1100 °C, while the FeO was determined by volumetric titration with $KMnO_4$ 10N in acid solution. Following petrochemical parameters have been calculated. Differentiation Index (sum of normative sialic minerals except the anortite); is calculated as D.I. = normative Q + Ab + Or + Ne + Kp + Lc. Solidification index by wt% is calculated as [S.I. = (MgO) / (MgO + FeO tot + Na_2O + K_2O)] and agpaitic Index was calculated as [A.I. = (Na_2O + K_2O) / Al_2O_3, in molecular terms].

4. Results

4.1 Petrographic and chemical analysis

The results of macroscopic and microscopic analysis of the samples highlight five main pyroclastic facies, belonging to the Oligo-Miocenic volcanic cycle (Columbu et al., 2011):

1) dark-purplish pyroclastics (FS) with medium to high welding degree (like-ignimbrite, WPR);

2) light-purplish pyroclastics (S) with medium to high welding grade (like-ignimbrite, WPR);

3) grey-greenish pyroclastics (P1) with medium-low welding (pumice-cineritic facies, UPR);

4) grey-greenish pyroclastics (P3) with same matrix as P1, but with higher lithic and pumice (pumice-cineritic facies, UPR);

5) grey-greenish pyroclastics (P2) with medium-low welding grade intermediate between P1 and P3, but with more similar characteristics to P1. Within these five groups the main differences are found between the strongly welded and welded purple pyroclastics (FS and S) and the low-welded grey-greenish pyroclastic facies (P1, P2, P3). The first are more homogeneous, compact, generally not altered; the latter are more heterogeneous, often more altered than purplish pyroclastics, with lithics in variable dimensions and sizes that affect their physical properties. According to macroscopic affinity and physical characteristics, it's therefore possible to group the five facies in two main groups: welded and strongly welded ignimbritic rocks (i.e. S and FS) and low-welded grey-greenish pyroclastic rocks (i.e. P1, P2, P3).

About chemical composition, the diagram of De La Roche et al. (1980) has been used to the classification, where:
R1 = 4 Si-11 (Na + K) -2 (Fe + Ti)
R2 = 6Ca + 2Mg + 2Al expressed in atoms per mole. As shown in Fig. 3, the rocks used in the construction of the tower can be classified as rhyodacites, rhyolites and subordinate dacites. Outcrop rocks have a similar classification. According to Middlemost diagram (1975; Fig. 4), which distinguishes sodium, potassium and potassium-rich series, the rocks of the tower and the outcrops fall among the potassium and potassium-rich series. According to the diagram of Peccerillo & Taylor (1976), the tower and outcrop samples fall between the high-potassium calcalkaline and shoshonitic series (Fig. 5).

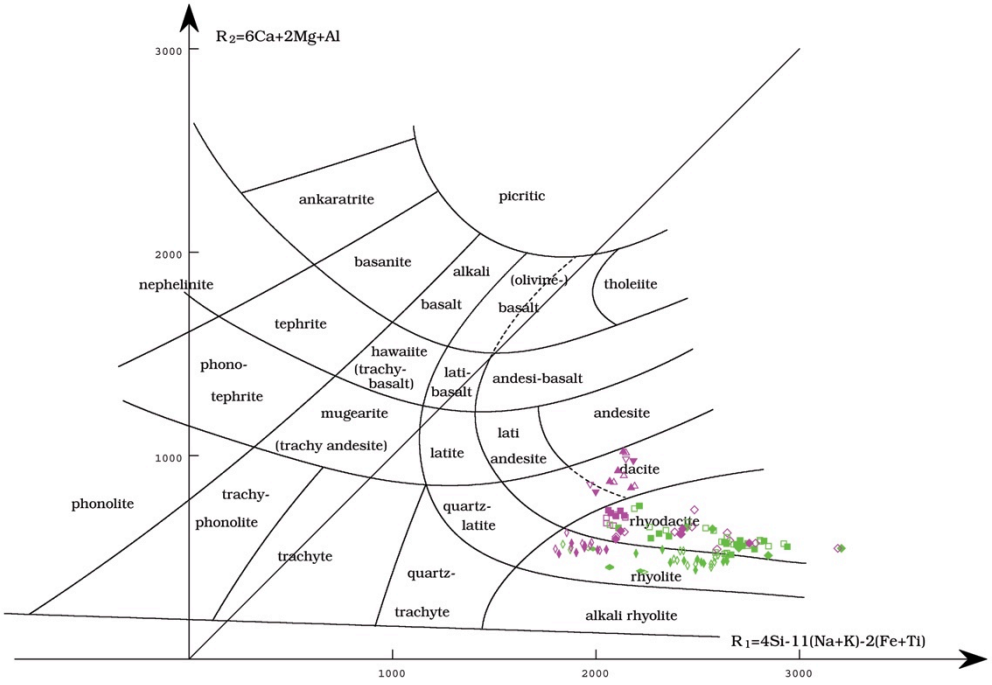

Fig. 3- De La Roche et al. (1980) classification diagram. Symbols of samples as caption of figure 4

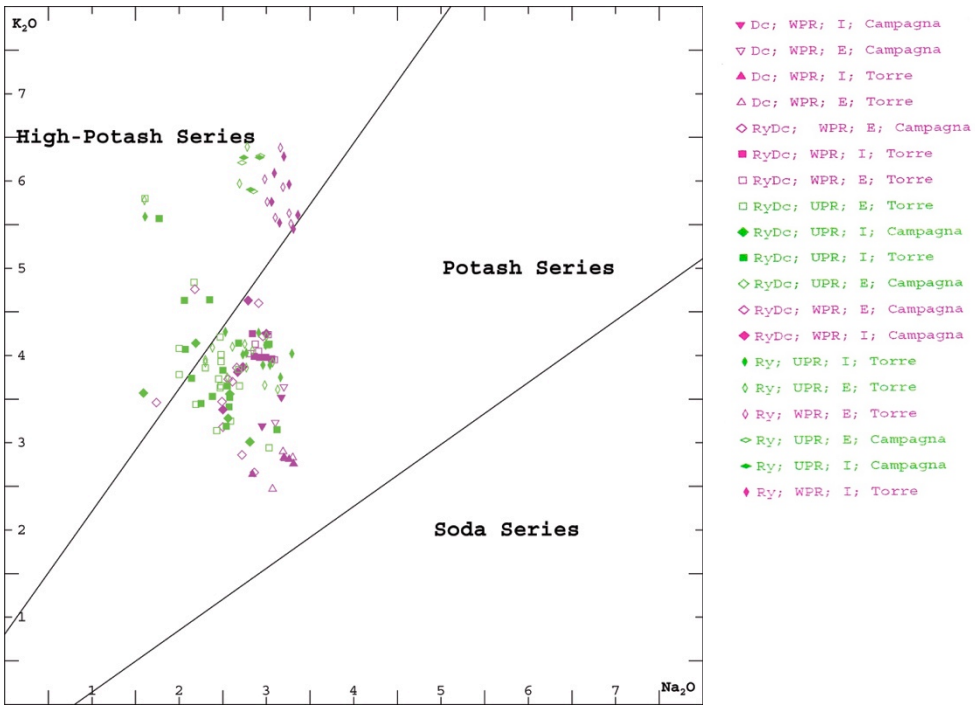

Fig. 4- Middlemost (1975) diagram. Symbols and means (classification according to De La Roche et al. 1980; see Fig. 3): Dc = dacite; Ry = rhyolite; RyDc = rhyodacite; Ry = rhyolite; Torre = tower; Campagna = field samples; I = inner sample (less altered); E = outer samples (more altered); WPR = Welded Pyroclastic Rocks (pinkish symbols); UPR = Unwelded Pyroclastic Rocks (green symbols)

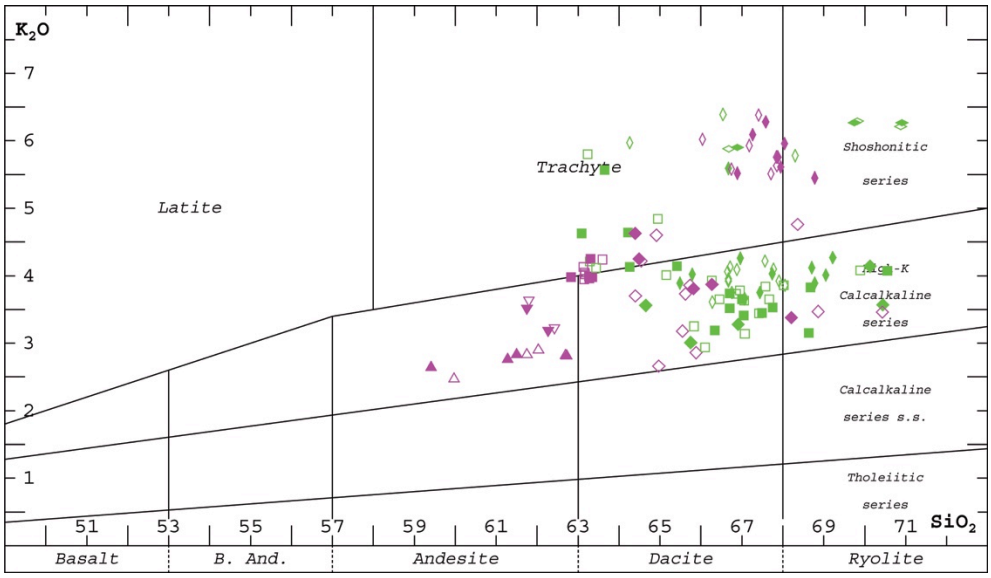

Fig. 5- Peccerillo and Taylor diagram (1976). Symbols of samples as caption of figure 4

4.2 Physical analysis

Of each sample taken from the tower, to highlight any differences, inner part (supposedly less altered) and the outer one directly in contact with the atmospheric agents, were separately analysed. The results, made by comparison of the 5 lithotypes identified through macroscopic and microscopic analysis, highlight 3 main populations with same physical behaviour (Fig. 6): strongly welded ignimbrites (FS, WPR); welded ignimbrites (S, WPR); low-medium welded pyroclastics (P1, P2, P3, pumice-cineritic facies, UPR).

He open porosity values of all the analysed pyroclastites show a broad variability between 5.3% and 46.4% with an average of 31.2% and a standard deviation of 7.3% (Figs. 6a, 6b).

Observing the graph Fig. 6a [where reposted He open porosity *versus* real density (ρ_R)] shows that the Welded Pyroclastic Rocks (WPR, inside the bordeaux circle in Fig. 6), represented by both strongly welded (FS) and welded (S) ignimbrites, have values of He open porosity between 5.3% and 32.3% and an average value of 22.5 ± 5.9%. The Unwelded Pyroclastic Rocks samples (UPR, inside the blue circle in Fig. 6), consisting of low-medium welded pyroclastites (P1, P2, P3) have He open porosity values varying from 30.8% to 46.4% and with an average value of 36.3 ± 2.6%. The bulk density, negatively related with the porosity, represents the degree of compactness of a rock and depends mainly on its structure, texture and real density of mineralogical phases (Figs. 6b, 6c).

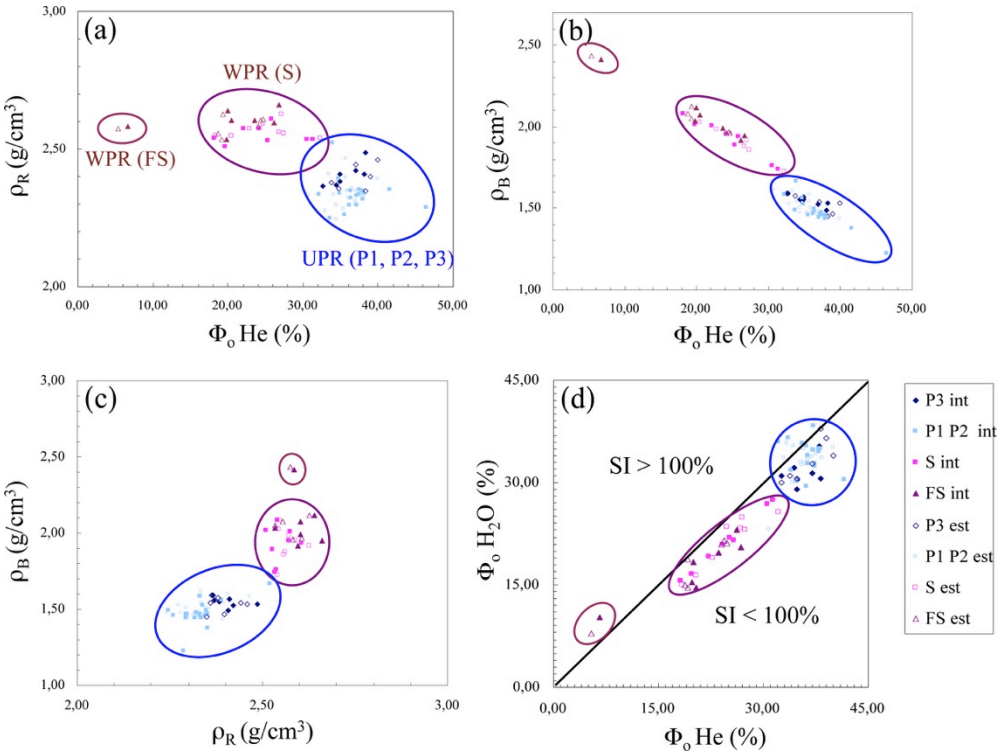

Fig. 6- Samples physical features: (a) He open porosity *vs* real density; (b) He open porosity *vs* bulk density; (c) real density *vs* bulk density; (d) He open porosity *vs* H_2O open porosity, with the solid black line of saturation index at 100% that divides the graphic in two fields. Symbols: int = inner samples; est = outer samples

UPR samples show a bulk density range from 1.22 to 1.66 g/cm^3, with an average of 1.50 ± 0.07 g/cm^3; WPR samples have bulk density between 1.72 and 2.44 g/cm^3, with an average of 1.99 ± 0.15 g/cm^3. The imbibition coefficient (CI_W%) generally shows a wide variability, closely related to open porosity, varying from a 3.2%, (with a corresponding open porosity of 5.3%) to 26.5% (with porosity of 37.1%).

The Fig. 6d shows the relation between H_2O and He open porosities, also highlighting indirectly the saturation index (S.I.%). This latter is often under the saturation line of 100%, but the FS-WPR samples and some UPR samples have values upper 100%, due to the anomalous behaviours of glassy matrix and/or the presence of hygroscopic phases (i.e. zeolites, phyllosilicates, salts).

Regarding physical-mechanical properties, the punching resistance index (Is_{50}) by PLT test generally shows a wide variability, ranging (for all samples analysed) from a minimum of 0.54 to a maximum of 5.3 MPa, with an average of 2.8 ± 1.1 Mpa, as function of welding of matrix, porosity and bulk density.

5. Discussion and conclusions

The work has allowed to define the petrographic and geochemical characteristics and the main physical-mechanical properties of pyroclastic used in the construction of the pentagonal tower of the Serravalle Castle and also, it suggests hypothesis of their provenance. The pyroclastic rocks show very different compositional and physical characteristics, imputable to several factors: volcanic deposition, welding degree, variable presence of glass and pumice, quantity and nature of lithic fragments, type and percentage of phenocrystals. These factors certainly also affected the geochemical features of the pyroclastites. According to observed petro-volcanological characteristics, they were divided into four main volcanic facies: 1) dark-purplish strongly welded ignimbrites (FS); 2) welded ignimbrites (S); 3) low-medium welded cineritic pyroclastites (P1, P2); 4) low-welded pumice-cineritic pyroclastites (P3).

Petrographic and geochemical data indicate that pyroclastic rocks have a variable composition: from dacite to rhyodacite to rhyolite (according to De La Roche et al. 1980). The Unwelded Pyroclastic Rocks (UPR samples: P1, P2 and P3 facies) show a more acid chemical composition.

The volcanics used for the construction of the tower have very petrographic and geochemical similarities with the rocks belonging to the *Piano e Multas* and *Turas* outcrops (for WPR ignimbrites) and to the outcrops of *Sa Sea* and *Monte Furru* (for UPR pyroclastites). These sectors could therefore represent the main supply areas of materials.

The characterization of physical properties (open porosity, bulk and real density, imbibition and saturation coefficients, punching resistance index) allowed to group the five lithotypes into two main distinct populations:

I) Welded Pyroclastic Rocks (WPR) with a different behaviour between strongly welded facies (FS) and welded facies (S), characterised by values of open porosity around 4-6% in first case, and 17-33% in second case; II) Unwelded Pyroclastic Rocks (UPR) represented by lithotypes P1, P2 and P3, with open porosity values between 31% and 47%.

Also the real density (affected by solid density and closed porosity) highlights a different behaviour between these two populations: WPRs samples have higher values with range from 2.51 to 2.66 g/cm^3, respect to 2.24-2.52 g/cm^3 of UPR. These differences are attributed to a higher amount of closed pores in UPRs samples, due to their cineritic-glassy matrix and wider presence of pumices. Moreover, P3 pyroclastics of UPR population show higher real density values than P1 and P2 pyroclastites, although having the same matrix composition and welding degree, due to a higher percentage of lithics which increases the real density values.

Observing the UPR pyroclastites with equal open porosity, it has been noted that the outer samples have on average higher values of the saturation index and imbibition coefficient than inner samples. This is also well highlighted by the water absorption kinetic, where WPR samples have lower water absorption velocities than UPR samples.

Due to their lower porosity and higher bulk density, WPR ignimbrites show greater physical-

mechanical strengths (i.e. resistance to puncture, Is_{50}) than UPR pyroclastites, in general with lower resistance in the outer samples than inner samples, indicating an increase of porosity in the outer portions due to a major alteration state. Due to different physical features, characterised by higher porosity and low mechanical resistance, the UPR pyroclastic facies (P1, P2, P3) show a greater decay, with the various macroscopic alteration forms: matrix decohesion, exfoliation, flaking, alveolation.

References

Angius V. (1831). In G. Casalis, *Dizionario Geografico-Storico-Statistico-Commerciale degli Stati di S.M. il Re di Sardegna, voce Bosa*.

Columbu S., Meloni P. (2015). *Alteration processes of geomaterials used on the pentagonal tower of Serravalle Castle (central-west Sardinia, Italy)*. Fortmed 2015, Universitat de València, Spain.

Columbu S., Garau A.M., Macciotta G., Marchi M., Marini C., Carboni D., Ginesu S., Corazza G. (2011). *Manuale sui materiali lapidei vulcanici della Sardegna centrale e dei loro principali impieghi nel costruito.* Iskra Edizioni, Ghilarza (OR), pp. 302.

De La Roche H., Leterrier J., Grandclaude P., Marchal M. (1980). *A classification of volcanic and plutonic rocks using R1-R2 diagram and major-element analyses - Its relationships with current nomenclature.* Chemical Geology, 29, 183-210.

Fara G. (1543). *Chorographia Sardiniae*. Sassari

Fiori G. (1995). *I Malaspina*, Ed. Tip.Le.Co. Piacenza

Franzini M., Leoni L. (1972). *A full matrix correction in X-ray fluorescence analysis*. Atti Soc. tosc. Sci. nat. Mem. Serie A 79 pp 7-22.

Franzini M., Leoni L., Saitta M. (1975). *Revisione di una metodologia analitica per fluorescenza-X, basata sulla correzione completa degli effetti di matrice.* Rend Soc Ital Min Petr 31(2). pp. 36-378.

Guagnini G. (1973). *I Malaspina*, Ed. Il Biscione, Milano.

Middlemost E.A.K. (1975). *The basalt clan*. Earth-Science Reviews, 11, 337-364.

Peccerillo A. & Taylor S.R. (1976). *Geochemistry of Eocene calc-alkaline volcanic rocks from the Kastamonu area, northern Turkey*. Contrib. Mineral. Petrol., 58, 63-81.

Scano D. (1936). *Castello di Bonifacio e Logudoro nella prima metà del XIII secolo*, in "Archivio Storico Sardo". pp. 11-52.

Soddu A. (2005). *I Malaspina e la Sardegna. Documenti e testi dei secoli XII-XIV*, Ed. Cuec, Cagliari.

Spanu S. (1981). *Il Castello di Bosa*. Ed. Spanu & C, Torino.